
# NQO1-Responsive Prodrug for in Cellulo Release of Cytochalasin B as Cancer Cell-Targeted Migrastatic

RESEARCH ARTICLE

NANO · MICRO small
www.small-journal.com

# NQO1-Responsive Prodrug for *in Cellulo* Release of Cytochalasin B as Cancer Cell-Targeted Migrastatic

*Mervic D. Kagho, Katharina Schmidt, Christopher Lambert, Lili Jia, Vignesh Venkatakrishnan, Luisa Mehr, Johan Bylund, Klemens Rottner, Marc Stadler, Theresia E. B. Stradal,* and Philipp Klahn**

**Migrastatic drugs targeting cell motility and suppressing invasiveness of solid tumors, have the potential to bring about a paradigm shift in the treatment of solid cancer. Cytochalasin B (CB) is a potent migrastatic compound, but its clinical use is limited by poor selectivity. Here, a NQO1-responsive prodrug, BQTML-CB is developed, synthesized in three steps from cytochalasin B derived from *Preussia similis* G22. BQTML-CB is selectively activated in NQO1-positive cancer cells, releasing active CB. *In vitro*, BQTML-CB significantly inhibits proliferation and migration in NQO1-positive U-2OS cells, causing actin disruption and cytokinesis abnormalities, while sparing NQO1-negative B16-F1 cells. The prodrug shows reduced effects on human neutrophils, indicating reduced immunosuppressive activity of BQTML-CB compared to CB. Co-culture studies reveal a beneficial bystander effect, as cleaved CB diffused into adjacent NQO1-deficient cells. These findings support BQTML-CB as a cancer-targeted prodrug with selective antiproliferative and migrastatic properties, highlighting the potential of C7-OH-modified cytochalasans in cancer therapy.**

## 1. Introduction

Cancer remains one of the leading causes of death and a significant global burden with over 10 million annual deaths worldwide.[1] In contrast to hematologic malignancies (involving the blood, bone marrow, and lymphatic system), predominantly characterized by uncontrolled clonal proliferation,[2,3] cells associated with solid tumors may invade the surrounding tissue and spread to other body parts (metastasis). This is believed to account for >90% of the observed mortality.[4,5] Conventional cytostatic anticancer therapies, on the other hand, primarily target cell proliferation, which makes up for the majority of treatment options currently available.[6]

In 2017, *Gandalovičová* et al. proposed the term "migrastatics" for anticancer drugs interfering with all modes of cancer cell invasiveness, including their ability to overcome the extracellular matrix (ECM) and establish secondary tumors.[6]

An anticancer therapy aiming toward migrastasis may potentially pose a paradigm change in solid cancer treatment,[10] as anti-metastatic agents[11] show synergistic effects with

M. D. Kagho, P. Klahn
Department of Chemistry and Molecular Biology
Division of Organic and Medicinal Chemistry
University of Gothenburg
Natrium, Medicinaregatan 7B, Gothenburg 413 90, Sweden
E-mail: philipp.klahn@gu.se

K. Schmidt, C. Lambert, L. Mehr, K. Rottner, T. E. B. Stradal
Department of Cell Biology
Helmholtz Centre for Infection Research
Inhoffenstrasse 7, 38124 Braunschweig, Germany
E-mail: theresia.stradal@helmholtz-hzi.de

C. Lambert, K. Rottner
Division of Molecular Cell Biology
Zoological Institute
Technische Universität Braunschweig
Spielmannstrasse 7, 38106 Braunschweig, Germany

The ORCID identification number(s) for the author(s) of this article can be found under https://doi.org/10.1002/smll.202410861



**DOI: 10.1002/smll.202410861**

C. Lambert, L. Jia, M. Stadler
Department of Microbial Drugs
Helmholtz Centre for Infection Research
Inhoffenstrasse 7, 38124 Braunschweig, Germany

V. Venkatakrishnan
Department of Life Sciences
Chalmers University of Technology
Kemivägen 4, Göteborg 41296, Sweden

J. Bylund
Department of Oral Microbiology and Immunology
Institute of Odontology
Sahlgrenska Academy
University of Gothenburg
Medicinaregatan 12F, Göteborg 413 90, Sweden

M. Stadler
Institute for Microbiology
Technische Universität Braunschweig
Spielmannstraße 7, 38106 Braunschweig, Germany

conventional therapies based on antiproliferation and cytotoxic effects.[12,13]

It was proposed that the selection pressure exerted by such agents may not cause resistance toward conventional therapies because the mechanisms targeted are of complete different nature.[10,14]

Potential targets for migrastatic anticancer therapies are those directly or indirectly associated with cell motility, i.e., affecting phenomena such as availability of ATP, mitochondrial metabolism, cytoskeletal dynamics, cell adhesion, cell polarization, ECM remodeling pathways, or cell contractility.[14,15] Actin plays a crucial role in most if not all motile processes of eukaryotic cells, including changes of cell shape, cell migration, vesicular trafficking, and cytokinesis.[16]

In this context, natural compounds interfering with actin polymerization and contractility, such as cytochalasans, jasplakinolide, latrunculins, staurosporine, and scytophycins have attracted particular research interest as potential migrastatics.[11,12,15]

Cytochalasans[17] are a large family of fungal secondary metabolites produced by many members across the Ascomycota, such as *Diaporthe* and *Chaetomium*.[18,19] Cytochalasans are biosynthesized in a concerted action by a fungal polyketide synthase and a non-ribosomal peptide synthetase (PKS-NRPS),[20] and commonly comprise a tricyclic structure consisting of an isoindolone core fused to a macrocyclic ring.[21,22] The structurally diverse family of cytochalasans displays a broad range of interesting biological activities,[23–25] but the most prominent activity of cytochalasans encountered in all cytochalasan subclasses is their inhibition of actin polymerization and/or disruption of actin filaments.[24,25]

Cytochalasans have demonstrated potent cytotoxic and antiproliferative effects against murine and human cancer cell lines,[20,21,25,26] likely due to their activity on actin. However, this bioactivity against actin is often viewed as a limiting factor for their broader applicability. Nevertheless, cytochalasin D (**CD**), a representative of the [11]cytochalasan subclass, and cytochalasin B (**CB**), a representative of the [14]cytochalasan sub class (**Figure 1**) have been studied for their anticancer activities early on. Their efficacy was investigated in vitro and in vivo,[26–31] with most studies focusing on **CB**, as it appears to be 20-fold less toxic than **CD** in mice.[31,32] Additionally and in contrast to **CD**, **CB** inhibits GLUT transporters[33] and potentially prevents glycolysis.[34–37] Glucose transporters have attracted a lot of interest as chemotherapeutic agents because most cancer cells rely primarily on high rates of glycolysis to maintain metabolic activity instead of relying on the potential for pyruvate oxidation in mitochondria to induce oxidative phosphorylation.[12,38] Thus, **CB** combines two favorable anticancer mechanisms. Finally yet importantly, in 2015 *Trendowski* et al. demonstrated synergistic potentiation of the microtubule binder paclitaxel and the topoisomerase inhibitor doxorubicin by **CB** in human ovarian carcinoma SKVLB1[13] as well as synergistic effects in vitro and in vivo in multi-drug resistant murine P388/ADR leukemia.[31]

The main challenge in designing cytochalasin B-based migrastatics lies in reducing systemic toxicity while enhancing selectivity for cancer cells. In 2015, *Waldmann* and co-workers demonstrated in a *de novo* synthesis approach of **CB**-inspired simplified analogs that actin disruption and cytotoxic effects can be conceptually decoupled.[7] The CB-analogues **1** and **2** (Figure 1B) resembled the characteristic architecture of the natural product at the scaffold level, yet were glucose import inhibitors only, not showing any actin binding. Recently, *Perlíková* and coworkers published CB-derived synthetic cytochalasan analogs **3**–**6** (Figure 1C), lacking the macrocyclic moiety but bearing aryl-containing side chains in the C10 position, which showed significantly reduced cytotoxicity against human BLM melanoma cells (at least twofold) and human MRC-5 fibroblasts (at least 185-fold) compared to **CB**.[8] The reported compounds retained some, albeit modest, bioactivity in an actin polymerization assay in vitro and on actin networks of living cells and exerted migrastatic activity in a spheroid invasion assay with BLM cells. Whether their compounds inhibited glucose import was not tested.

Although their results indicated that migrastatic and antiproliferative activities can be uncoupled – which offers promising prospects for further development of cytochalasin analogs as migrastatics – the drastic reduction of unwanted migrastatic activity of these compounds on non-cancer cells might also limit their potential on cancer cells.

We do need to consider that targeting actin cytoskeleton dynamics and/or contractility affects many processes in both cancer and non-cancer cells, such as cell migration, division, and exocytosis. Additionally, it has been shown that systemic administration of **CB** induces immunosuppression in in vivo murine tumor models,[30] potentially affecting immune processes by interfering with both mesenchymal and amoeboid migration of leukocytes.

Thus, migrastatic effects need to be confined and selective for cancer cells, which seems to be even more important than the reduction of specific antiproliferative activity.

In this context, the flavin-containing quinone reductase NQO1 (NAD(P)H quinone oxidoreductase 1) has received a lot of attention as target for the conversion of prodrugs to increase selectivity of anticancer therapies[39,40] and biomarker tumor-specific activation of imaging probes.[40,41] NQO1 is found in almost all mammals. It catalyzes the two-electron reduction of quinones into hydroquinones by using either NADPH or NADH as electron donors and FMN as prosthetic group.[41,42] NQO1 is constitutively expressed at relatively low levels in a variety of healthy tissues under physiological conditions, with over 90% localized in the cytosol.[42] It has been shown that expression of NQO1 is highly up-regulated in solid tumors such as cholangiocarcinoma, breast, cervical, and lung cancers, and that elevated levels of NQO1 are associated with cancer progression, metastasis,[43,44] and bad prognosis for patients.[41,42]

Here, we report the design, synthesis, and in vitro evaluation of the bioresponsive prodrug **BQTML-CB** (**Scheme 1**), a semi-synthetic derivative aimed at directing the migrastatic activity of cytochalasin B (**CB**) toward cancer cells over-expressing the quinone-oxidoreductase NQO1. This approach is shown to increase the selectivity of **BQTML-CB** for NQO1-expressing cancer cells.

## 2. Results and Discussion

### 2.1. SAR and Design of BQTML-CB

Cytochalasans such as **CB**[45–47] as well as numerous other cytochalasans[21,48–63] have been targeted by elegant total synthesis campaigns for more than40 years.[21,22,64–67] However, so

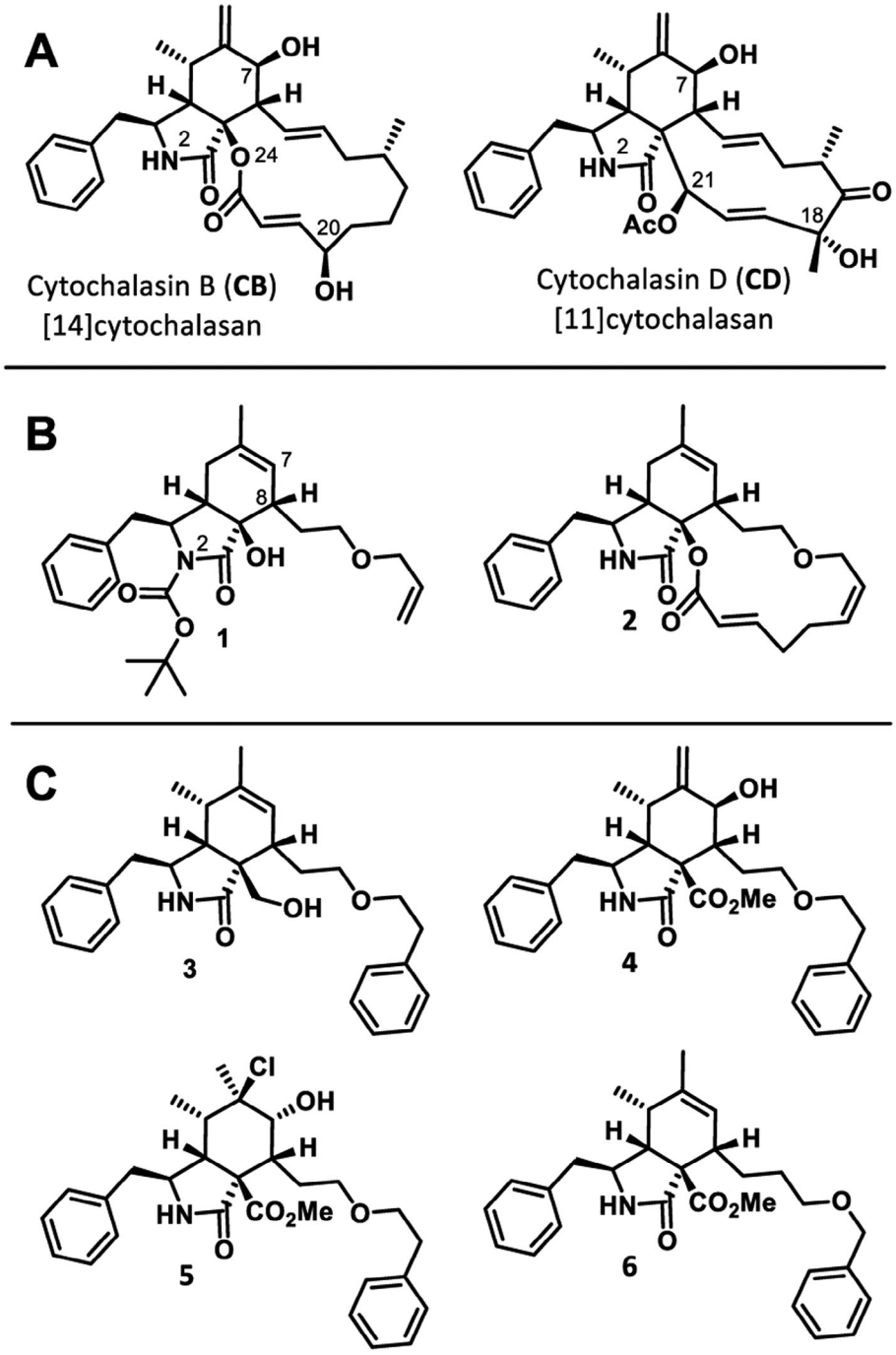


**Figure 1.** A) Structures of cytochalasin B (**CB**) and cytochalasin D (**CD**). B) cytochalasin B-inspired analogs by *Waldmann* and co-workers.[7] C) Cytochalasan analogs lacking the macrocyclic moiety reported by *Perlíková* and co-workers.[8] Atom numbering follows the nomenclature for cytochalasans introduced by *Binder* et al.[9]

far, total synthesis routes are lengthy and expensive in terms of time and low overall yield,[68] failing to supply sufficient amounts of cytochalasans for derivatization campaigns. Even the synthesis of the structurally simplified CB analogs **3–6** (Figure 1C) requires at least 10–13 steps from commercially available starting materials and provides in overall yields between 1% and 2%.[8]

In contrast, availability has improved in recent years due to mass production via exploitation of fungal producers,[69,70] establishment of mutasynthesis approaches,[71] and PKS-NRPS engineering[72] of certain cytochalasan-producing biosynthetic gene clusters. **CB** can be obtained in sufficient amounts in batch fermentations using submerged cultures in shaking flasks of the endophytic fungus *Preussia similis* G22 (DSM32328), as

 

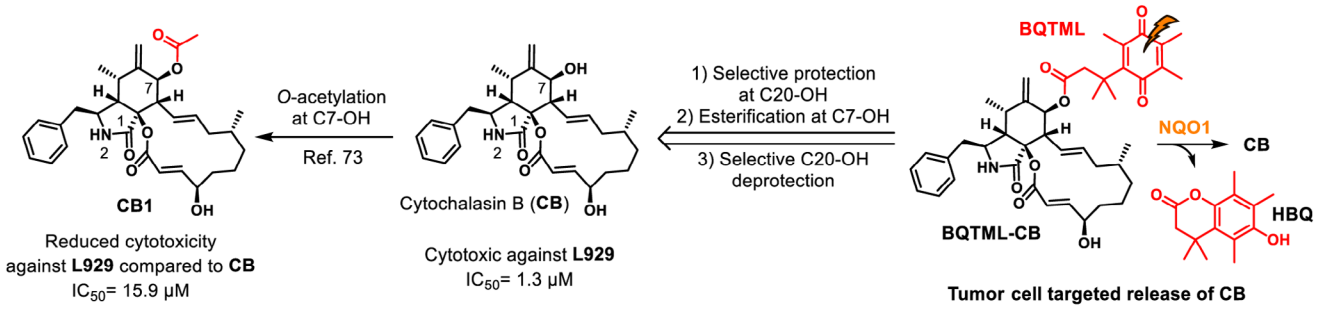


**Scheme 1.** Structures of cytochalasin B (**CB**) and its derivative **CB1** and **BQTML-CB**.

described by *Kretz* et al.[24,73] This allows for the exploration of semi-synthetic modifications of **CB** delivering fermentation yields after purification of 200 mg/10 L formation batch.

In our recent work,[73] we shed light on the structure-activity relationship of **CB** on actin by virtual docking and semi-synthetic modification. We found that **CB** occupies the same binding pocket *in silico* as **CD** when docked onto non-polymerizable, monomeric G-actin (PDB: 3EKU),[74] although binding less tightly to actin as the larger macrocycle of the [14]cytochalasin **CB** does not allow to penetrate as deeply into the binding pocket as **CD**, resulting in a reduced hydrogen bridge network for **CB**. We also determined the importance of the C7-OH function of **CB** for its actin binding activity. We were able to show that **CB1** (Figure 1), a semi-synthetic derivative of **CB**, obtained by *O*-acetylation of the hydroxyl group at C7-OH position of the 6-membered ring, exhibited a significantly reduced cytotoxic activity against mouse connective tissue fibroblasts L929 with an $IC_{50}$ value of 15.9 µM versus 1.3 µM for **CB**. In addition, a high dose treatment of human osteosarcoma cells (U-2OS) with **CB1** showed no impact on their filamentous actin (F-actin) network, as opposed to the high dose treatment with **CB** leading to complete collapse of the latter, indicating the importance of this moiety for actin interaction.[73]

Identifying the same binding pocket for **CD** and **CB**,[73] we hypothesized that the attachment of larger groups to the C7-OH position would further reduce both, cytotoxic as well as migrastatic activity, similar to photoactivatable probes of **Nvoc-CD** (structure shown in Supporting Information) published as preprint earlier by *Nair* et al.[75]

In order to confine **CB**'s migrastatic and cytotoxic properties to tumor cells, we envisaged to introduce a bulky benzoquinone Trimethyl-Lock (BQTML)[76] ester responsive to the tumor-associated enzyme NQO1 to the C7-OH position of **CB**.[77] Thus, in the resulting **BQTML-CB** (Scheme 1) the C7-OH would be masked, reducing actin binding and cytotoxicity significantly, while upon tumor-associated presence of NQO1 the reductive, autoimmolative release of **CB** (and the corresponding BQTML-derived hydrobenzoquinone **HBQ**, Scheme 1) is envisaged unfolding its migrastatic and cytotoxic activity in a selective manner. BQTML esters are known to be serum stable due to their high steric hindrance of the three pendant methyl groups and have been extensively used in the development of chemical probes that target NQO1.[76,78,79]

### 2.2. Semi-Synthesis of BQTML-CB

To prove our concept, we aimed to semi-synthesize the antimetastatic prodrug **BQTML-CB** starting from **CB** obtained by fermentation of *Preussia similis* G22 (DSM 32 328) as described by *Kretz* et al.[24,73]

BQTML carboxylic acid **7** was synthesized via a two-step sequence (**Scheme 2**) following a slightly modified procedure described previously by *Rohde* et al.[80] First, a *Friedel–Crafts* type condensation of commercially available 2,3,5-trimethyl-1,4-benzenediol (**8**) with 3-methyl-2- butenoic acid methyl ester (**9**) in methanesulfonic acid at 70 °C furnished the hydrobenzoquinone **HBQTML** in 70% yield. Subsequent oxidation with *N*-bromosuccinimide at 23 °C gave BQTML carboxylic acid **7** in 96% yield.

In parallel, as described earlier by us,[73] the treatment of **CB** with TBSCl in the presence of imidazole and DMAP at 40 °C, resulted in a selective *O*-silylation of the C20-OH group to afford compound **10** in 85% yield (**Scheme 3**). This allows for the selective esterification of the C7-OH function.

Therefore, compound **7** was activated with EDCI·HCl in the presence of a stoichiometric amount of DMAP and imidazole in anhydrous $CH_2Cl_2$ for 30 min and coupled to the C7-OH forming BQTML-ester **11** in 70% yield. Finally, the desired **BQTML-CB** was accessed by cleaving the C20-OTBS group with a 1 M-solution of TBAF in 70% yield as outlined in Scheme 3.

### 2.3. In Vitro Activation of BQTML-CB in the Presence of Human NQO1

With the prodrug **BQTML-CB** in hand, we next investigated the release of **CB** in the presence of commercially available human NQO1 (recombinantly expressed in *E. coli*) by LC-MS analysis. **BQTML-CB** was incubated with NQO1 in the presence of required co-factors NADH and FMN in TRIS buffer (20 mM, pH 7.4) at 37 °C and after removing the enzyme by

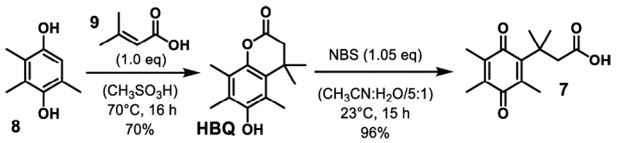


**Scheme 2.** Synthesis of the BQTML carboxylic acid **7**.

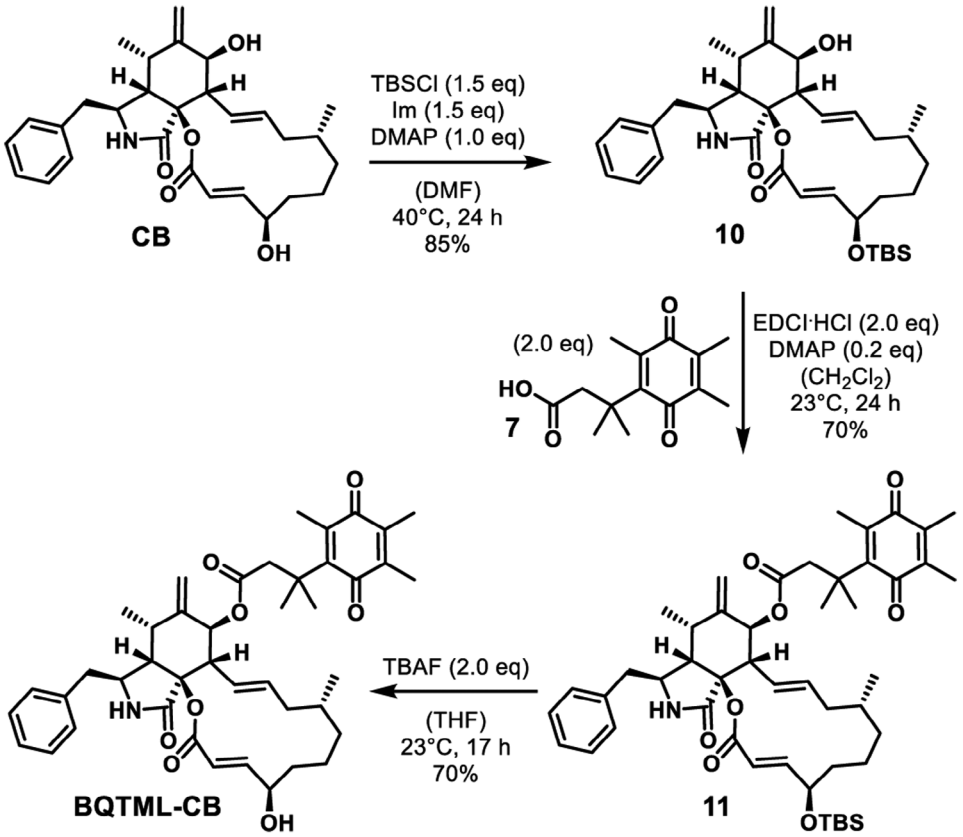


**Scheme 3.** Semi-synthesis of **BQTML-CB**.

10 kDa cut-off spin columns we analyzed the solution by LC-MS (**Figure 2**). **BQTML-CB** (Figure 2 B1: $R_t$ = 5.15 min and C1: mass 710 m/z for $[M-H]^-$) was completely converted into **CB** (Figure 2 B4: $R_t$ = 3.71 min and C2: mass 480 m/z for $[M-H]^+$) and **HBQ** (Figure 2 B4: $R_t$ = 3.51 min and C3: mass 235 m/z for $[M-H]^+$) within 10 min at 37 °C. No intermediate **HBQTML-CB** (Figure 2A) was observed. The conversion was dependent on the presence of NQO1 as well as the co-factors NADH and FMN. In the absence of either of them, no conversion was observed.

### 2.4. Identification of BQTML-CB Processing Cell Lines

Next, we screened for **BQTML-CB** responding and non-responding cell lines. We tested four wild type cell lines, namely human osteosarcoma cells (U-2OS), mouse melanoma cells (B16-F1), mouse fibroblasts (NIH 3T3), and rat fibroblasts (Rat2) available in our lab for NQO1 expression by western blot analysis. NQO1 expression was detected in U-2OS, NIH 3T3, and -to a lesser extent- in Rat2 cell lysates, but not in B16-F1, which fits extant literature reports describing B16-F1 as NQO1-deficient cell line (see Figure S1, Supporting Information).[77]

Interestingly, we observed slightly different apparent molecular weights of the bands presumed to represent NQO1 protein in each case. Stored mass data at NCBI (human: NP_000894.1, mouse: NP_032732.3, rat: NP_058696.2), however, indicated a consistent mass of 31 kDa for all three species. This observation could be indicative of distinct post-translational modifications in the cell lines used or, alternatively, a lack of specificity of the used primary antibody.

To confirm that the detected protein band indeed corresponds to NQO1 in each case, we conducted knockdown experiments in U-2OS, NIH 3T3, and Rat2 cells. Following siRNA transfection targeting NQO1 mRNA, we observed a significant reduction in NQO1 signal in all cell lines, verifying that these protein signals indeed corresponded to NQO1 (see Figure S2, Supporting Information). To qualitatively assess if the selected NQO1 expressing and non-expressing cell lines were capable of cleaving and activating **BQTML-CB**, we strived to re-extract the compounds from spiked growth media following 3 h exposition to cells (**Figure 3**).[73] No-treatment controls were used to exclude instability and decomposition of **BQTML-CB** to **CB** over time in growth medium.

Two peaks were identified and shown to correspond to **BQTML-CB** (711 Da, Rt = 8.25 min, III) and **CB** (479 Da, Rt = 14.5 min, II) in all extracts and a minor peak in extracts derived from U-2OS (Figure 3C), NIH 3T3 (Figure 3D), and Rat2 (Figure 3F) cells potentially representing the cleaved **HBQ** (236 Da, Rt = 7.75 min, I; Figure 3). Extracts of medium controls (Figure 3A and B) and B16-F1 (Figure 3E) showed scant amounts of **CB**, probably representing impurities derived from previous preparative purification steps. Summarizing, we confirmed the conversion of **BQTML-CB** to **CB** and **HBQ** in the presence of U-2OS,

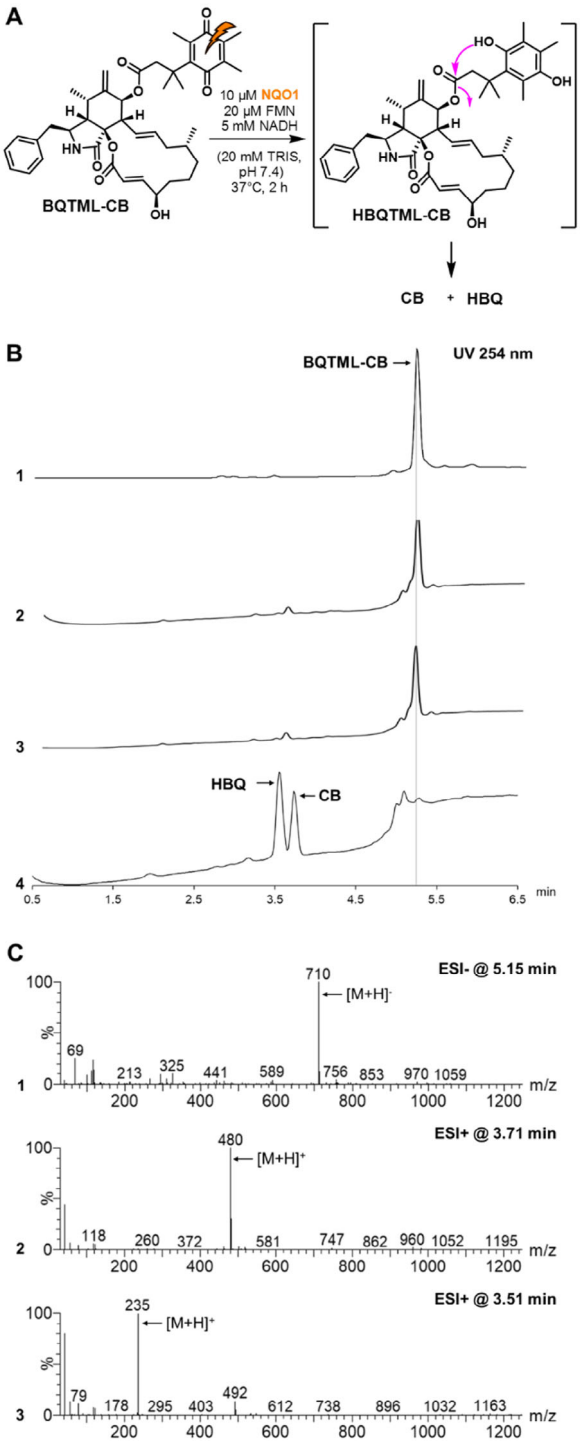


**Figure 2.** A) Mechanism of NQO1-mediated release of **CB** and **HBQ**. B) UV chromatogram at 254 nm of (**B1**): **BQTML-CB** (500 µM) in TRIS buffer (20 mM, pH 7.4), (**B2**): **BQTML-CB** (500 µM) after 10 min incubation with FMN (20 µM) and NADH (5 mM) in TRIS buffer (20 mM, pH 7.4) at 37 °C. (**B3**): **BQTML-CB** (500 µM) after 10 min incubation with human NQO1 (10 µM) in TRIS buffer (20 mM, pH 7.4) at 37 °C. (**B4**): **BQTML-CB** (500 µM) after 10 min incubation with human NQO1 (10 µM), FMN (20 µM), NADH (5 mM) in TRIS buffer (20 mM, pH 7.4) at 37 °C. C) $ESI^-$ or $ESI^+$ mass spectra of (**C1**): **B1** @5.15 min, (**C2**): **B4** @4.72 min, and (**C3**): **B4** @3.51 min.

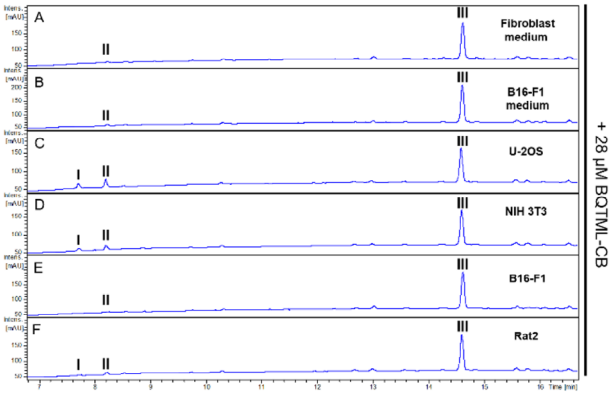


**Figure 3.** UV chromatograms of re-extraction experiments at 210 nm. Fibroblast and B16-F1 medium were supplemented with 28 µM **BQTML-CB** and supplied to U-2OS (**C**), NIH 3T3 (**D**), B16-F1 (**E**), and Rat2 cells (**F**) or sustained in a cell-free environment as controls (**A** and **B**) for 3 h under cell culture conditions. Re-extractions were performed from removed media using 2 mL EtOAc and extracts subsequently measured by HPLC-MS. Distinct peaks correspond to **BQTML**-derived hydrobenzoquinone **HBQ** (I), **CB** (II), and **BQTML-CB** (III) identified from their respective mass spectra (see Figure S3, Supporting Information).

NIH 3T3 and – to a somewhat lesser extent – Rat2 cells, whereas **BQTML-CB** remained stable following exposure to B16-F1 cells.

Despite the high sequence identity and structural similarity between human, rat, and mouse NQO1 (mouse/human 86%; mouse/rat 94%; human/rat 86%),[81] studies have consistently shown that rodent NQO1 exhibits a higher rate of quinone substrate reduction compared to its human counterparts.[82,83] This makes it highly unlikely that the lack of **BQTML-CB** conversion in murine B16-F1 cells is due to slower conversion by murine NQO1.

### 2.5. Characterization of BQTML-CB on Cell Proliferation and the Actin Cytoskeleton

With these first results at hand, we proceeded with the characterization of **BQTML-CB** on the cellular level by performing a 24 h proliferation assay. Here, the four cell lines were treated with an initial concentration of 4.2 µM **BQTML-CB** – referring to the previously determined $IC_{50}$ concentration of **CB**[73] – and DMSO as vehicle control. Proliferation was analysed using the IncuCyte S3 *Adherent Cell-by-Cell* module of its Live Cell Analysis Software (**Figure 4**). A commercial **CB** standard was utilized in low (1.3 µM) and high (6.3 µM) concentrations, allowing the comparison of bioactivity of released and activated **CB**. Significantly, reduced proliferation of U-2OS cells after **BQTML CB** treatment similar to low dose treatment with **CB** was observed (Figure 4A,E), whereas **BQTML-CB**-treated B16-F1 cells were nearly unaffected (Figure 4B,E).

In contrast, NIH 3T3 and Rat2 cells by trend, but not in statistically significant fashion, showed impaired proliferation (Figure 4C–E). In addition, morphological alterations like flattening, rounding, and cell grouping were noted for U-2OS and NIH 3T3 following 24 h **BQTML-CB** treatment (Figure 4A,C; see representative phase contrast images).

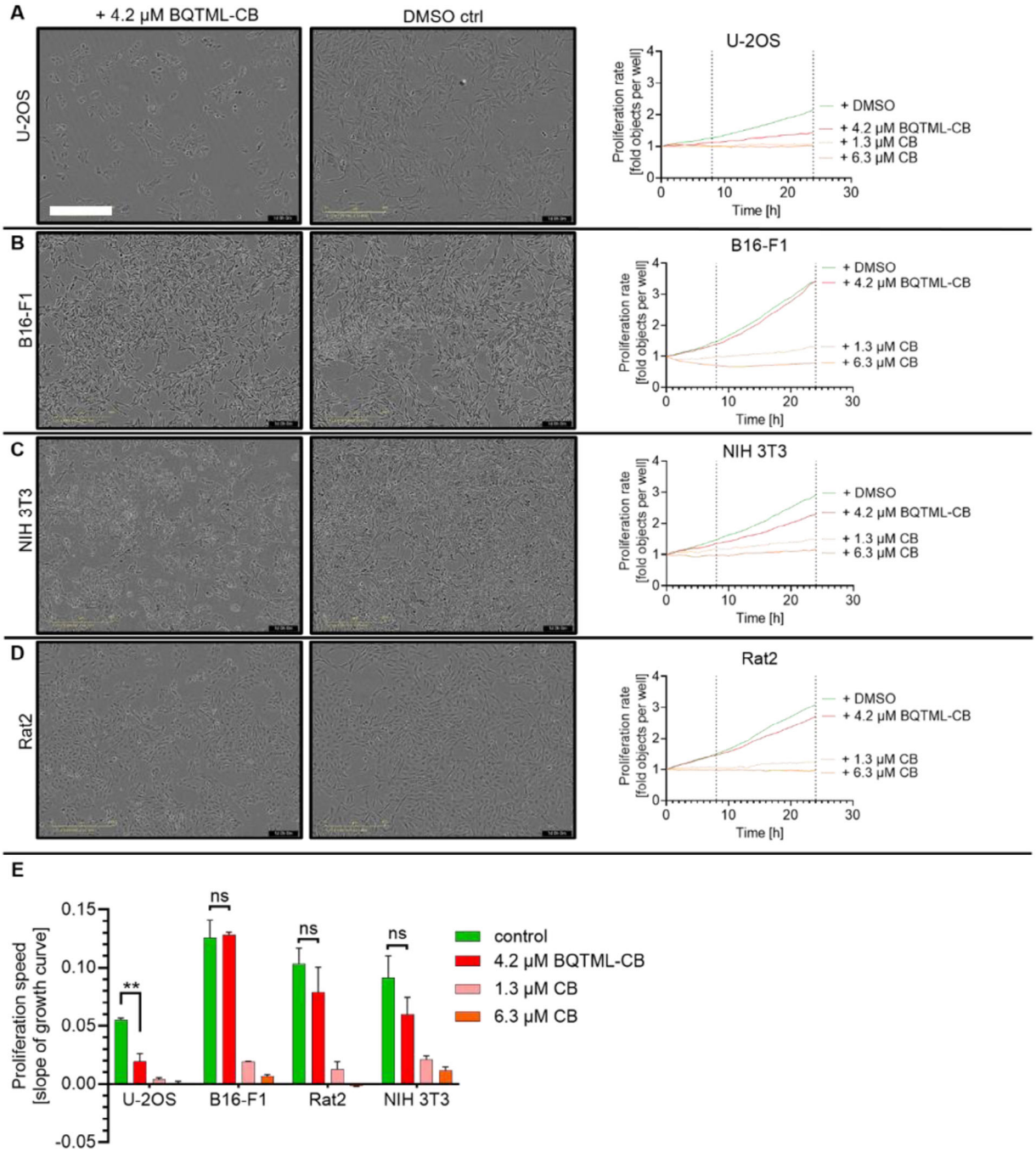


**Figure 4.** Analysis of cell proliferation during 24 h BQTML-CB treatment. Phase contrast images of U-2OS (A), B16-F1 (B), NIH 3T3 (C), and Rat2 (D) cells recorded following 24 h treatment with 4.2 µM BQTML-CB and DMSO as vehicle control. The proliferation rate was assessed by automated cell counting for 24 h. The graphs (right panels) show mean phase object counts from at least two independent experiments with two replicates each were plotted over time. The Representative scale bar in (**A**) valid for subpanels **A–D** in (**A**) corresponds to 400 µM. (E) Normalized proliferation speed determined by calculation of slopes from respective growth curves between 8 and 24 h following treatment start (see dotted lines in **A–D**). Bars represent means + SEM; $n = 2$, $^{**}p < 0.0014$ (tested by ordinary one-way ANOVA).

As cell grouping is a common indicator for diminished cell motility and since **CB** is well-known and utilized as versatile actin assembly inhibitor, we next strived to find **CB** concentrations causing morphological alterations and actin inhibition phenotypes as similar as possible to those seen with **BQTML-CB**. This would allow roughly estimating **CB** concentrations in action in cells following conversion by respective, endogenous NQO1. First, we performed a cell proliferation assay, treating the four cell lines with increasing concentrations of **CB**, ranging from 0.02 to 1.3 µM (**Figure 5**). Here, we observed initial signs of

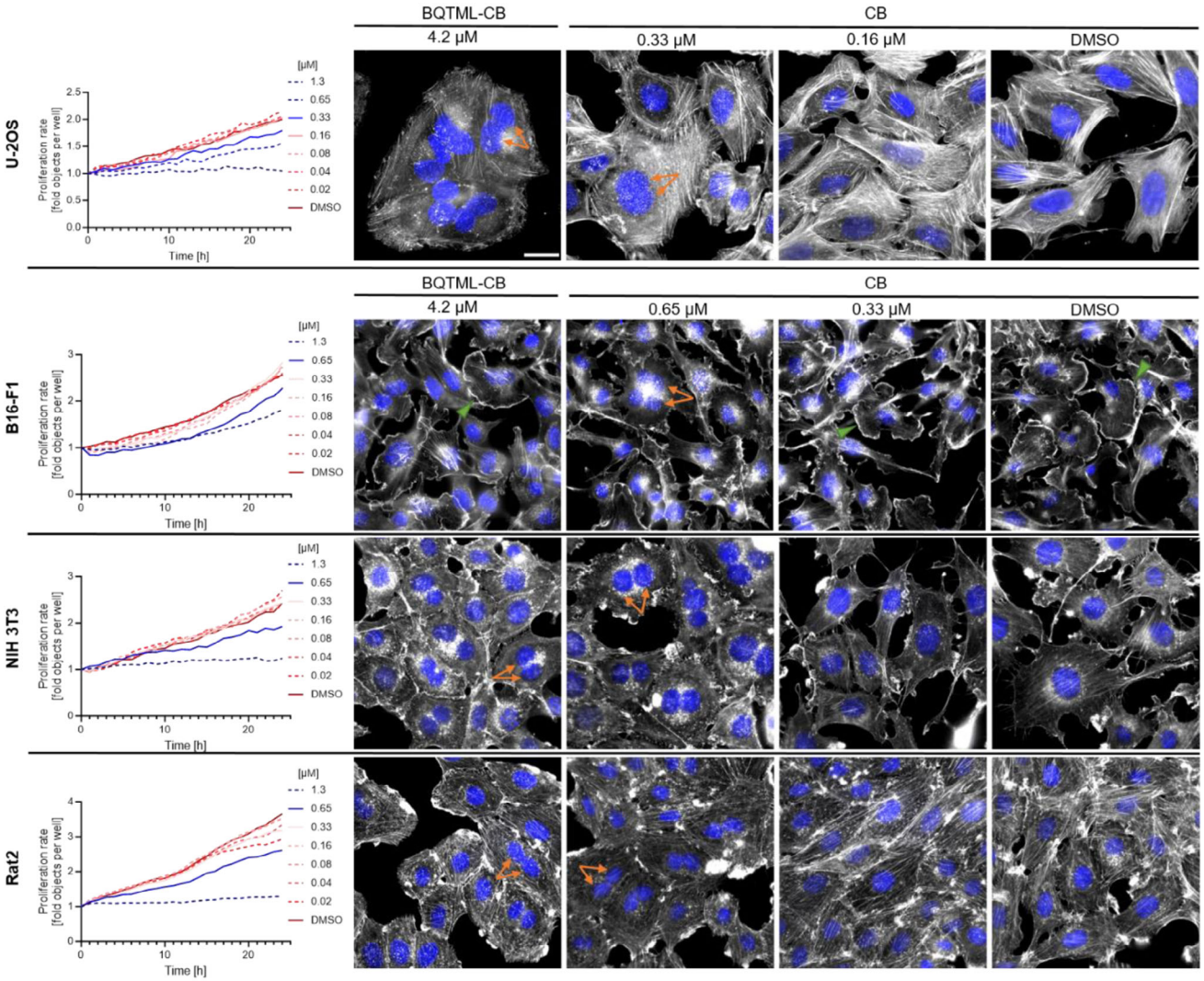


**Figure 5.** Estimation of active concentration ranges of **CB** required to obtain characteristic long-term alterations on cellular morphologies, in particular multinucleation, in U-2OS, B16-F1, NIH 3T3, and Rat2 after treatment with 4.2 µM **BQTML-CB** for 24 h. The respective cell lines were treated with gradually increasing **CB** concentrations, ranging from 0.02 to 1.3 µM, as well as DMSO as vehicle control. Proliferation rates were calculated by plotting measured cell counts against time for each concentration and cell line. The resulting growth curves were color-clustered based on similarities to DMSO control (red and orange lines) or hampering effects on cell growth (blue lines). Here, the highest **CB** concentration comparable to DMSO control (continuous orange line) and the lowest **CB** concentration affecting cell growth (continuous blue line) were utilized to choose appropriate **CB** concentrations in future experiments. Specifically, cells were treated as indicated with 0.65 or 0.33 µM (= lowest concentration showing first growth inhibitory effects) and 0.33 or 0.16 µM (= highest concentration comparable to DMSO control), fixed, and stained for F-actin using fluorescent phalloidin-AF488 (grayscales) and nuclear DNA using DAPI (pseudo colored in blue). Representative overlay images of each treatment condition were shown combined with images of **BQTML-CB** treated cells for comparison. Double arrows highlight the characteristic hallmark of **CB** long-term effects – multinucleated cells – whereas the green arrowheads mark lamellipodial structures still observable in **BQTML-CB**-treated B16-F1 cells. The representative scale bar corresponds to 25 µM.

impaired cell growth upon 0.33 µM **CB** treatment in U-2OS and 0.65 µM **CB** in the other three cell lines (Figure 5, graphs on the left). Based on these concentrations, we proceeded with a well-established actin disruption assay to visualize potential morphological alterations of the cytoskeleton.[24] Briefly, the four cell lines were seeded onto fibronectin-coated coverslips and treated with i) 4.2 µM **BQTML-CB**, ii) the minimal **CB** concentration required for effects on proliferation determined above in comparison to iii) the highest **CB** concentration not yet exerting on effects on the actin cytoskeleton, as well as iv) DMSO as vehicle control.

This will allow estimating the range of **CB** concentrations potential seen after **BQTML-CB** conversion in each cell line. After 24 h incubation, the cells were fixed and stained for F-actin using fluorescently coupled phalloidin (Figure 5). Staining revealed high numbers of multinucleated U-2OS cells concomitant with enlarged cell size, diminished lamellipodial protrusions – F-actin rich structures at the cell periphery considered as hallmarks of protrusion – and a largely intact stress fiber network – contractile, anti-parallel F-actin bundles – upon **BQTML-CB** treatment. These effects were comparable to treatment with 0.33 µM **CB** (Figure 5). Similar subcellular responses were seen for NIH 3T3

 

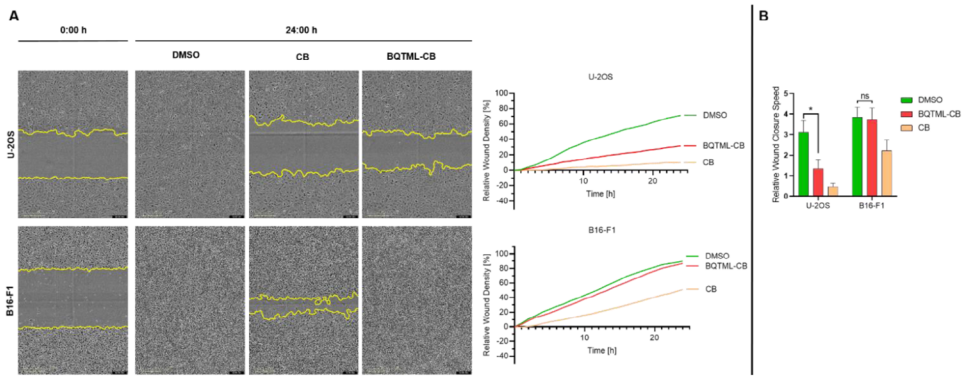


**Figure 6.** Wound scratch assay to study the migration properties of U-2OS and B16-F1 cells in **BQTML-CB** treatment conditions. (A) Phase contrast images of U-2OS (upper panel) and B16-F1 (lower panel) recorded at time points 0 and 24 h after treatment with DMSO as vehicle control, 1.3 μM **CB**, and 4.2 **μM BQTML-CB**. The relative wound density [%] was assessed by automated calculation of the scratch wound using the *Scratch Wound Analysis* module of the IncuCyte *Live Cell Analysis* software for 24 h and plotted against time. (B) Relative wound closure speed was determined by calculating the slopes from the respective relative wound density curve between 0 and 24 hours. Data are means + SEM; $n = 3$, * $p < 0.0415$, ordinary one-way ANOVA.

cells, but accompanied by less dramatic cell size enlargement. Effects on NIH 3T3 were thus more reminiscent of a treatment with 0.65 μM **CB** (Figure 5). In contrast, multinucleation induced by **BQTML-CB** treatment in Rat2 cells appeared less pronounced than in aforementioned cell lines. Here, actin staining revealed a largely intact actin network, but a striking increase of peripheral F-actin accumulations compared to DMSO control, representing ruffle-like structures. This particular response was comparable to that seen with 0.65 μM **CB** (Figure 5). The impact of **BQTML-CB** on B16-F1 cells was mostly indiscernible from DMSO control, as expected, with at best minimal effects on the efficiency of formation of pronounced lamellipodia. Of note and as opposed to **BQTML-CB**, lamellipodia formation was already partially compromised with as low as 0.33 μM **CB**, and even more so with 0.65 μM, with the latter concentration also already inducing occasional multinucleation (Figure 5). Based on these results, it is quite likely that the potential release of **CB** in **BQTML-CB**–treated cells induced the described cellular effects – multinucleation, cell size enlargement, and actin reorganization in U-2OS, NIH 3T3 and Rat2 cells – and was causative for their impaired cell proliferation. Actin reorganization, multinucleation and cellular enlargement are well-documented hallmarks of **CB** bioactivity that is linked to the inhibition of F-actin and the F-actin-containing contractile ring, ultimately disturbing cytokinesis,[84,85] and impairing proliferative capabilities, as especially shown for U-2OS cells over the course of this study. NQO1 expression differs across the cell lines surveyed here, with U-2OS and NIH 3T3 showing ample levels, followed by Rat2, while B16-F1 cells were shown to be virtually devoid of NQO1 expression. This fits reasonably well with the less dramatic Rat2 cell enlargement and impairment of proliferation upon **BQTML-CB** as compared to U-2OS, and the absence of this phenotype in B16-F1, best explained by a potentially lower and no conversion of **BQTML-CB** to **CB** in Rat2 and B16-F1 cells, respectively. To exclude that the mild effects in Rat2 and B16-F1 can be explained by a potentially reduced sensitivity of these cell lines against **CB**, we additionally determined their respective $IC_{50}$ values. These cytotoxic values ranged from 0.27 μM (NIH 3T3), 0.58 μM (U-2OS) and 0.75 μM (Rat2) to 1.88 μM in B16-F1 cells (see Table S2, Supporting Information). Notably, we also tested the low cytotoxicity-derivative **CB1** in U-2OS cells, which displayed an $IC_{50}$ of more than 20x higher than **CB**, consistent with previous data[73] (see Table S2, Supporting Information). Furthermore, whereas B16-F1 cells are indeed somewhat less sensitive to **CB** than the other lines tested, their growth was nonetheless blocked with the **CB** concentrations used in the proliferation assay (1.3 μM), but not with the much higher concentration of **BTQML-CB** (4.2 μM). This thus corroborates the notion that B16-F1 cells cannot convert **BTQML-CB** to release **CB**.

### 2.6. Characterization of BQTML-CB as Potential Migrastatic

To further characterize the migrastatic activity of **BQTML-CB**, we implemented a Wound Scratch Assay[86,87] based on the protocol of the *IncuCyte Scratch Wound 96-Well Real-Time Cell Migration Assay*. In this assay, migration of cells into a wound previously scratched into the cell monolayer is visualized by time-lapse microscopy.

As U-2OS and B16-F1 were identified as responsive and non-responsive to **BQTML-CB**, and NQO1-expressing and non-expressing cell lines, respectively, we decided to focus on the two of them. Frankly, both were seeded onto coated *96-Well Imagelock Plates* and grown overnight until reaching nearly 100% confluence. After the wound scratch, cells were treated with 1.3 μM CB, 4.2 μM **BQTML-CB**, and DMSO as vehicle control and afterward recorded and analyzed using the *IncuCyte Scratch Wound* module (**Figure 6**). After 24 h, the relative wound density of NQO1-expressing U-2OS cells treated with **BQTML-CB** and **CB** comprised 32% and 10%, respectively, and was thus considerably lower in both cases than DMSO control (70%). In contrast, B16-F1 were unaffected in the presence of **BQTML-CB**, exhibiting a relative wound density of 87%, i.e., virtually identical to DMSO control (90%), whereas **CB** markedly reduced the wound density to 40% in this cell line. These results confirm that the observed disruption of the F-actin cytoskeleton by **BQTML-CB** in NQO1-expressing cell lines (as observed above) does correlate with impairment of cell migration, while NQO1 non-expressing cells

lacking the ability to convert the prodrug to **CB** remain largely unaffected. Thus, the migrastatic activity of **BQTML-CB** is indeed NQO1-dependent.

### 2.7. Impact of BQTML-CB on Neutrophils

Neutrophils are one example of immune cells the functions of which are largely dependent on actin dynamics and that would be highly risky to affect with migrastatic drugs. To investigate the impact of **BQTML-CB** on human neutrophils and assess a potential immunosuppressant activity as shown for **CB**,[30] we measured extracellular reactive oxygen species (ROS) production by isoluminol-enhanced chemiluminescence[88] after addition of *N*-formylmethionyl-leucyl-phenylalanine (fMLF) in the presence and absence of **CB** or **BQTML-CB** (**Figure 7**). When neutrophils are stimulated with high dose of the potent chemoattractant fMLF, formyl peptide receptor 1 (FPR1) triggers activation of the NADPH-oxidase resulting in release of ROS.[89,90] This activation results in a robust ROS response from cells with an onset of seconds, a peak in minutes, and termination in roughly 5 min (see Figure 7, *Buffer control*). The termination of FPR1 signaling depends on coupling of the receptor to the F-actin cytoskeleton; in the presence of **CB**, the response is both increased and strongly prolonged.[91] In contrast, in the presence of **BQTML-CB**, no such effect was observed, and the fMLF-response highly similar to that in the buffer control (Figure 7; Figure S4, Supporting Information). These results clearly indicate that **BQTML-CB** is not converted into **CB** and does not interfere with the F-actin cytoskeleton in human neutrophils.

To further support this conclusion, we performed a neutrophil migration assays[92] utilizing fMLF (10 nM) as chemoattractant. The cells were incubated in the absence or presence of **CB** and **BQTML-CB** for 5 min at 37 °C and cell migration through a membrane with pores of 3 µm in size was allowed for 90 min at 37 °C. Afterward, cells that had migrated below the filter were visualized microscopically and quantified by a lactate dehydrogenase activity assay of lysates (**Figure 8**). While in the absence of these compounds, a mean of ≈85% of the neutrophils migrated, the presence of **CB** significantly impaired cell migration.

In contrast, in the presence of **BQTML-CB** at concentrations of both, 7.0 and 0.7 µM, cell migration showed no statistically significant reduction. These data allow concluding that no significant conversion of **BQTML-CB** to **CB** in human neutrophils is occurring and point toward a substantially reduced immunosuppressant activity of **BQTML-CB**.

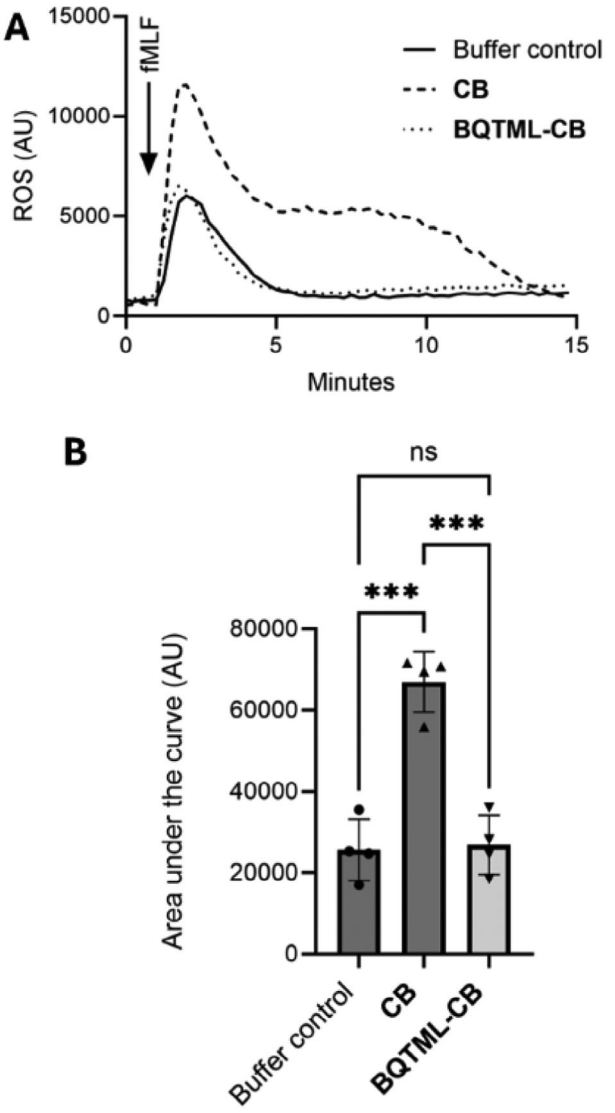


**Figure 7.** Measurement of extracellular ROS by isoluminol-enhanced chemiluminescence,[88] from isolated human neutrophils after addition of fMLF (100 nM; arrow) in presence and absence of **CB** (10.9 µM) and **BQTML-CB** (7 µM). (A) The fMLF response from one biological replicate (= cells from one donor) with all samples run in technical triplicates (mean values given) is shown. (B) The fMLF response, quantified as AUC-values from ROS measurements, from 4 biological repeats (cells from 4 different blood donors, see also Figure S4, Supporting Information). Individual values (means of three technical repeats) and mean ±SEM are shown. Statistical analysis performed was One-way ANOVA followed by Tukey's multiple comparisons test.

## 3. Conclusion

In summary, we successfully converted the potent cytostatic cytochalasin B (**CB**) into the NQO1-responsive prodrug **BQTML-CB**. **BQTML-CB** by semi-synthesis in an efficient three-step sequence, starting with **CB** obtained from the endophytic fungus *Preussia similis* G22 (DSM 32 328). In addition, we identified one NQO1-negative (B16-F1) and three NQO1 positive cell lines – namely U-2OS, NIH 3T3, and Rat2 – able to convert **BQTML-CB** and yield the active actin inhibitor **CB** and its side product **HBQ**.

Our results clearly demonstrated that NQO1-mediated release of active **CB** causes dramatic effects on cell proliferation accompanied by typical characteristics of disturbed cytokinesis induced by **CB**, such as multinucleation, actin disruption, and cell type-dependent cell enlargement, with most prominent effects observed for the osteosarcoma-derived cell line U-2OS. As NQO1 is described to be overexpressed in cancer cell lines compared to healthy tissues,[93] we also confirmed that proliferation of immortalized, but non-cancer-derived cell lines, such as NIH 3T3 and Rat2 (both fibroblast lines), were not as prominently affected by the compound, despite their capability to process **BQTML-CB** to some extent. Furthermore, wound scratch assays in cultures of

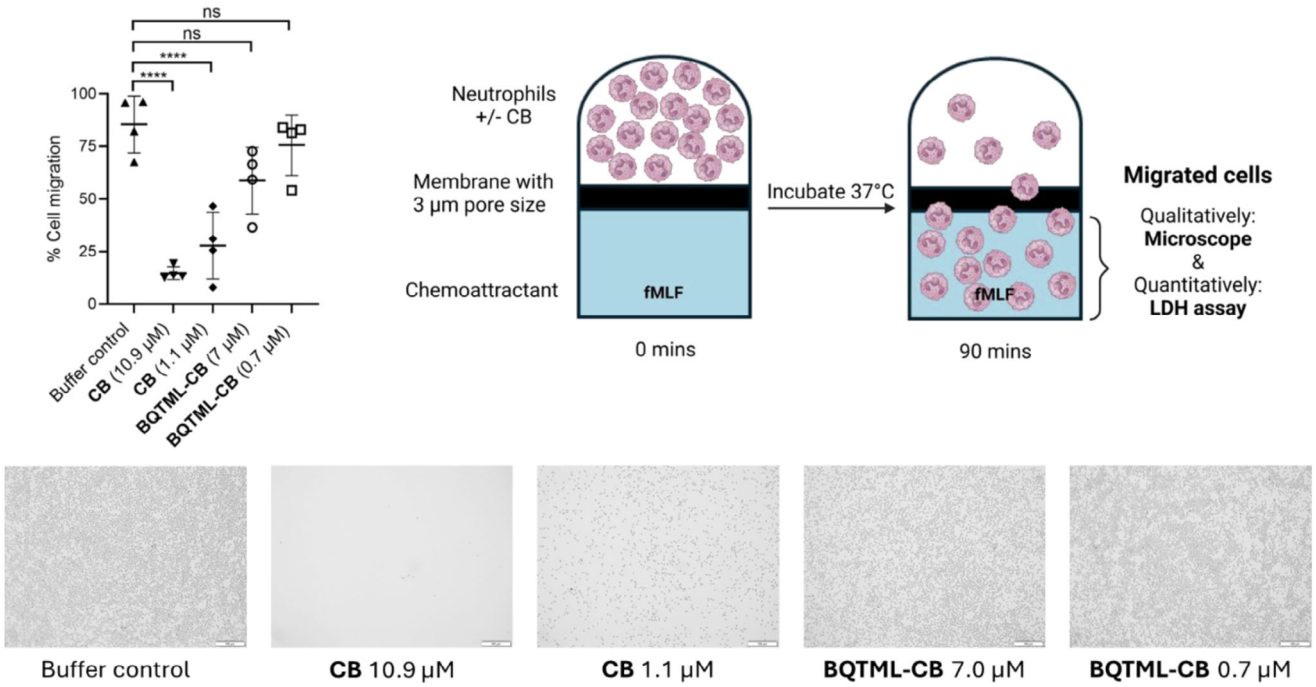


**Figure 8.** Measurement of neutrophil migration in response to fMLF. Cells were put on top of filters in the presence or absence of **CB** (10.9 and 1.1 µM,) and **BQTML-CB** (7.0 and 0.7 µM), incubated for 5 min before chemoattractant (fMLF, 10 nM) was added to the wells below the filter. After 90 min at 37 °C, cells that migrated into the lower compartments were visualized by microscopy and then quantified by measuring lactate dehydrogenase (LDH) activity in lysates. Data shown are representative micrographs (lower panel) and means from 4 biological repeats (cells from 4 different blood donors) each in technical triplicates. Statistical analysis performed was One-way ANOVA followed by Tukey's multiple comparisons test.

U-2OS and B16-F1 cells clearly demonstrated that the migrastatic activity of **BQTML-CB** is NQO1-dependent, as cell migration was clearly impaired in NQO1-positive U-2OS cells, while no effect was observed for NQO1-negative B16-F1 cells.

Finally, the production of FPR1-mediated, extracellular reactive oxygen species (ROS) in human neutrophils in the presence of **BQTML-CB** clearly revealed that the compound, in distinct contrast to parent **CB**,[91] does also not interfere with the F-actin cytoskeleton of human neutrophils. This was further supported by **CB**, but not **BQTML-CB** dramatically reducing cell migration in human neutrophils. All these data suggest a diminished immunosuppressant activity of **BQTML-CB** compared to **CB**.

Thus, our newly developed prodrug **BQTML-CB** harbors the potential of a cancer-targeting migrastatic, with distinct activities on cancer cell proliferation and migration, while leaving non-cancer cells, including important reactive cells of our immune systems, such as the human neutrophils tested here, unaffected.

To test the applicability of the compound in a slightly more realistic experimental scenario with diverse cell types, we co-cultured the **BQTML-CB**-responsive U-2OS with non-responsive B16-F1 cells (see Figure S5, Supporting Information). This led to astonishing effects on the F-actin cytoskeleton in B16-F1 cells, being disrupted in a fashion comparable to **CB** treatments (compare with Figure 5). **CB** is well known to be membrane-permeable, and it is reasonable to assume that the cleaved and activated **CB** can diffuse into surrounding cells and affect even NQO1-deficient cells like, in this case, B16-F1. Considering the high cellular heterogeneity of tumors,[94] such bystander effects[95,96] might be beneficial to a certain extent to prevent tumor migration. However, to improve the selectivity of cytochalasan-based prodrugs for targeted cancer cells, one way to go might be to modify the prodrug in a way that the cargo remains inside the target cell post-cleavage. Aside from manipulation of membrane permeability, cytochalasans reported as being irreversible, such as deoxaphomin[97] and pseudofuscochalasin A[98] could also represent interesting candidates for **BQTML** coupling in this context. However, the precise molecular mechanism mediating irreversibility of these compounds on actin organization is still subject of active, current investigation.[25] Specifically, irreversibility would have to be driven by compound immobilization at respective sites of action, in order for this approach to confine effects to distinct target cells. Taken together, we conclude that modification of the C7-OH position, as is the case for **BQTML-CB**, to generate tumor-targeted prodrugs indeed represents a suitable strategy to harness the migrastatic activity of cytochalasans such as **CB**.

## Supporting Information

Supporting Information is available from the Wiley Online Library or from the author.

## Acknowledgements

The authors gratefully acknowledge the German Research Foundation (DFG) for research funding through the CytoLabs consortium (DFG Research Unit FOR 5170, grants KL 3012/4-1 (P.K.), RO 2414/12-1 (K.R.),

 

STR 666/10-1 (T.S.) and STA 1282/8-1 (M.S.)). The project was further financially supported by the starting funds of P.K. at the University of Gothenburg. J.B. thanks the Swedish Research Council (VR 2022-00561) and King Gustav V Memorial Foundation for financial support. The authors are also thankful to SciLifeLab research infrastructure, in particular the Swedish NMR Center (SNC, GU) and the Proteomics Core Facility (PCF, GU), for analytical support. The content of this work is solely the responsibility of the authors and does not necessarily represent the official views of the funding agencies.

## Conflict of Interest

The authors declare no conflict of interest.

## Author Contributions

M.D.K. and K.S. contributed equally to this work. Contributions are given with CRediT definition according to *Brand* et al.:[104] Conceptualization was performed by P.K. and T.E.B.S.; Methodology was performed by M.D.K, K.S., and V.V.; Software development and validation were performed by M.D.K., K.S., and V.V.; Formal analysis was performed by M.D.K., K.S., C.L., L.M., and V.V.; Investigation was performed by M.D.K., K.S., C.L., V.V., and L.J.; Resources was performed by P.K., T.E.B.S, K.R., M.S., and J.B; Data curation was performed by P.K.; Writing—original draft by M.D.K., K.S., C.L., V.V., T.E.B.S., and P.K.; Writing—review & editing by all authors; Visualization was performed by P.K., K.S., V.V., and M.D.K; Supervision was performed by P.K., T.E.B.S., K.R., J.B., and M.S.; Project administration: M.D.K., K.S., V.V., P.K., and T.E.B.S.; Funding acquisition by P.K., T.E.B.S., K.R., M.S., and J.B.

## Data Availability Statement

The data that support the findings of this study are openly available in NMRxiv at https://doi.org/10.57992/nmrxiv.p77, reference number 77.

## Keywords

cytochalasin B, migrastatics, NQO1, prodrugs

Received: November 14, 2024
Revised: March 7, 2025
Published online: March 17, 2025

[1] H. Sung, J. Ferlay, R. L. Siegel, M. Laversanne, I. Soerjomataram, A. Jemal, F. Bray, *CA. Cancer J. Clin.* **2021**, *71*, 209.
[2] J. Prick, G. de Haan, A. R. Green, D. G. Kent, *Exp. Hematol.* **2014**, *42*, 841.
[3] P. C. Nowell, *Science* **1976**, *194*, 23.
[4] H. Dillekås, M. S. Rogers, O. Straume, *Cancer Med.* **2019**, *8*, 5574.
[5] J. Fares, M. Y. Fares, H. H. Khachfe, H. A. Salhab, Y. Fares, *Signal Transduct. Target. Ther.* **2020**, *5*, 28.
[6] A. Gandalovičová, D. Rosel, M. Fernandes, P. Veselý, P. Heneberg, V. Čermák, L. Petruželka, S. Kumar, V. Sanz-Moreno, J. Brábek, *Trends Cancer* **2017**, *3*, 391.
[7] M. Sellstedt, M. Schwalfenberg, S. Ziegler, A. P. Antonchick, H. Waldmann, *Org. Biomol. Chem.* **2015**, *14*, 50.
[8] B. Formánek, D. Dupommier, T. Volfová, S. Rimpelová, A. Škarková, J. Herciková, D. Rösel, J. Brábek, P. Perlíková, *RSC Med. Chem.* **2024**, *15*, 322.
[9] M. Binder, C. Tamm, W. B. Turner, H. Minato, *J. Chem. Soc. Perkin Trans. 1* **1973**, *11*, 1146.
[10] D. Rosel, M. Fernandes, V. Sanz-Moreno, J. Brábek, *Trends Cancer* **2019**, *5*, 755.
[11] S. Gayan, S. Doshi, T. Dey, in *Handbook Oxidative Stress Cancer Ther. Asp*, Springer Nature Singapore, Singapore **2022**, 3157.
[12] M. Trendowski, *Biochim. Biophys. Acta – Rev. Cancer* **2014**, *1846*, 599.
[13] M. Trendowski, T. D. Christen, C. Acquafondata, T. P. Fondy, *BMC Cancer* **2015**, *15*, 632.
[14] M. Raudenská, K. Petrláková, T. Juriňáková, J. Leischner Fialová, M. Fojtů, M. Jakubek, D. Rösel, J. Brábek, M. Masařík, *Trends Cancer* **2023**, *9*, 293.
[15] A. Gandalovičová, D. Rosel, J. Brábek, in *Approaching Complex Diseases*, vol. *2*, (Ed.: M. Bizzarri), Springer, Cham, **2020**, pp. 203–211.
[16] K. Rottner, J. Faix, S. Bogdan, S. Linder, E. Kerkhoff, *J. Cell Sci.* **2017**, *130*, 3427.
[17] M. Binder, C. Tamm, *Angew. Chem., Int. Ed.* **1973**, *12*, 370.
[18] C. Chepkirui, M. Stadler, *Mycol. Prog.* **2017**, *16*, 477.
[19] M. Stadler, J. Fournier, D. N. Quang, A. Y. Akulov, *Nat. Prod. Commun.* **2007**, *2*, 287.
[20] E. Skellam, *Nat. Prod. Rep.* **2017**, *34*, 1252.
[21] K. Scherlach, D. Boettger, N. Remme, C. Hertweck, *Nat. Prod. Rep.* **2010**, *27*, 869.
[22] S. Bräse, A. Encinas, J. Keck, C. F. Nising, *Chem. Rev.* **2009**, *109*, 3903.
[23] K. T. Yuyama, L. Wendt, F. Surup, R. Kretz, C. Chepkirui, K. Wittstein, C. Boonlarppradab, S. Wongkanoun, J. Luangsa-ard, M. Stadler, W.-R. Abraham, *Biomolecules* **2018**, *8*, 129.
[24] R. Kretz, L. Wendt, S. Wongkanoun, J. Luangsa-ard, F. Surup, S. Helaly, S. Noumeur, M. Stadler, T. Stradal, *Biomolecules* **2019**, *9*, 73.
[25] C. Lambert, K. Schmidt, M. Karger, M. Stadler, T. E. B. Stradal, K. Rottner, *Biomolecules* **2023**, *13*, 1247.
[26] M. Trendowski, *Anticancer Agents Med. Chem.* **2015**, *15*, 327.
[27] P. F. Bousquet, L. A. Paulsen, C. Fondy, K. M. Lipski, K. J. Loucy, T. P. Fondy, *Cancer Res.* **1990**, *50*, 1431.
[28] M. R. Steiner, B. Altenburg, C. S. Richards, J. P. Dudley, D. Medina, J. S. Butel, *Cancer Res.* **1978**, *38*, 2719.
[29] D. Medina, C. J. Oborn, B. B. Asch, *Cancer Res.* **1980**, *40*, 329.
[30] D. Bogyo, S. R. E. Fondy, L. Finster, C. Fondy, S. Patil, T. P. Fondy, *Cancer Immunol. Immunother.* **1991**, *32*, 400.
[31] M. Trendowski, J. M. Mitchell, C. M. Corsette, C. Acquafondata, T. P. Fondy, *Invest. New Drugs* **2015**, *33*, 290.
[32] J. Singh, R. D. Hood, *Teratology* **1987**, *35*, 87.
[33] K. Kapoor, J. S. Finer-Moore, B. P. Pedersen, L. Caboni, A. Waight, R. C. Hillig, P. Bringmann, I. Heisler, T. Müller, H. Siebeneicher, R. M. Stroud, *Proc. Natl. Acad. Sci. U. S. A.* **2016**, *113*, 4711.
[34] S. H. Zigmond, J. G. Hirsch, *Science* **1972**, *176*, 1432.
[35] C. Y. Jung, A. L. Rampal, *J. Biol. Chem.* **1977**, *252*, 5456.
[36] A. L. Rampal, H. B. Pinkofsky, C. Y. Jung, *Biochemistry* **1980**, *19*, 679.
[37] H. B. Pinkofsky, D. S. Dwyer, R. J. Bradley, *Life Sci.* **1999**, *66*, 271.
[38] E. S. Reckzeh, H. Waldmann, *ChemBioChem* **2020**, *21*, 45.
[39] X. Yang, J. Duan, L. Wu, *Future Med. Chem.* **2022**, *14*, 363.
[40] A. E. M. A. Khan, V. Arutla, K. S. Srivenugopal, *Cells* **2024**, *13*, 1272.
[41] Z. Cheng, W. O. Valença, G. G. Dias, J. Scott, N. D. Barth, F. de Moliner, G. B. P. Souza, R. J. Mellanby, M. Vendrell, E. N. da, S. Júnior, *Bioorg. Med. Chem.* **2019**, *27*, 3938.
[42] K. Zhang, D. Chen, K. Ma, X. Wu, H. Hao, S. Jiang, *J. Med. Chem.* **2018**, *61*, 6983.
[43] H. Asgharian, L. Chen, L. Fish, A. Navickas, J. Yu, B. Woo, A. S. Nanda, B. Choi, S. Zhou, J. Rabinowitz, H. Goodarzi, *Nat. Cancer* **2023**, *4*, 682.
[44] X. Wang, Y. Liu, A. Han, C. Tang, R. Xu, L. Feng, Y. Yang, L. Chen, Z. Lin, *Oncogene* **2022**, *41*, 5107.
[45] G. Stork, Y. Nakahara, Y. Nakahara, W. J. Greenlee, *J. Am. Chem. Soc.* **1978**, *100*, 7775.

[46] G. Stork, E. Nakamura, *J. Am. Chem. Soc.* **1983**, *105*, 5510.
[47] A. M. Haidle, A. G. Myers, *Proc. Natl. Acad. Sci. USA* **2004**, *101*, 12048.
[48] C. Tian, X. Lei, Y. Wang, Z. Dong, G. Liu, Y. Tang, *Angew. Chem., Int. Ed.* **2016**, *128*, 7106.
[49] M. Zaghouani, C. Kunz, L. Guédon, F. Blanchard, B. Nay, *Chem. - Eur. J.* **2016**, *22*, 15257.
[50] S. M. Canham, L. E. Overman, P. S. Tanis, *Tetrahedron* **2011**, *67*, 9837.
[51] J. Reyes, N. Winter, L. Spessert, D. Trauner, *Angew. Chem., Int. Ed.* **2018**, *57*, 15587.
[52] D. Lücke, Y. Linne, K. Hempel, M. Kalesse, *Org. Lett.* **2018**, *20*, 4475.
[53] E. Merifield, E. J. Thomas, *J. Chem. Soc. Perkin Trans. 1* **1999**, 3269.
[54] X. Long, Y. Ding, H. Wu, J. Deng, *Synlett* **2020**, *31*, 301.
[55] H. Dyke, R. Sauter, P. Steel, E. J. Thomas, *J. Chem. Soc. Chem. Commun.* **1986**, 1447.
[56] H. Dyke, P. G. Steel, E. J. Thomas, *J. Chem. Soc. Perkin Trans. 1* **1989**, 525.
[57] B. M. Trost, M. Ohmori, S. A. Boyd, H. Okawara, S. J. Brickner, *J. Am. Chem. Soc.* **1989**, *111*, 8281.
[58] E. Vedejs, J. G. Reid, *J. Am. Chem. Soc.* **1984**, *106*, 4617.
[59] E. Vedejs, J. D. Rodgers, S. J. Wittenberger, *J. Am. Chem. Soc.* **1988**, *110*, 4822.
[60] K. S. Yeung, I. Paterson, *Angew. Chem., Int. Ed.* **2002**, *41*, 4632.
[61] M. Zaghouani, O. Gayraud, V. Jactel, S. Prévost, A. Dezaire, M. Sabbah, A. Escargueil, T. L. Lai, C. Le Clainche, N. Rocques, S. Romero, A. Gautreau, F. Blanchard, G. Frison, B. Nay, *Chem. - Eur. J.* **2018**, *24*, 16686.
[62] E. J. Thomas, J. W. F. Whitehead, *J. Chem. Soc., Chem. Commun.* **1986**, 727.
[63] E. Merifield, E. J. Thomas, *J.Chem.Soc., Chem. Commun.* **1990**, 464.
[64] Y. Y.-L. Zhao, X.-W. X. Long, H. Wu, J. Deng, *Org. Chem. Front.* **2022**, *9*, 6979.
[65] H. Zhang, J. Zhang, R. Bao, C. Tian, Y. Tang, *Tetrahedron Chem* **2022**, *2*, 100022.
[66] H. Zhu, C. Chen, Q. Tong, Y. Zhou, Y. Ye, L. Gu, Y. Zhang, in Progress in the Chemistry of Organic Natural Products, (Eds.: A. Kinghorn, H. Falk, S. Gibbons, Y. Asakawa, J.-K. Liu, V. M. Dirsch), Springer, Cham, **2021**, pp. 1-134.
[67] X. Long, H. Wu, Y. Ding, C. Qu, J. Deng, *Chem* **2021**, *7*, 212.
[68] K. Speck, T. Magauer, *Beilstein J. Org. Chem.* **2013**, *9*, 2048.
[69] C. Lambert, L. Shao, H. Zeng, F. Surup, P. Saetang, M. C. Aime, D. R. Husbands, K. Rottner, T. E. B. Stradal, M. Stadler, *Mycologia* **2023**, *115*, 277.
[70] B. M. Kemkuignou, C. Lambert, K. Schmidt, L. Schweizer, E. G. M. Anoumedem, S. F. Kouam, M. Stadler, T. Stradal, Y. Marin-Felix, *Fitoterapia* **2023**, *166*, 105434.
[71] C. Wang, C. Lambert, M. Hauser, A. Deuschmann, C. Zeilinger, K. Rottner, T. E. B. Stradal, M. Stadler, E. J. Skellam, R. J. Cox, *Chem. – A Eur. J.* **2020**, *26*, 13578.
[72] C. Wang, V. Hantke, R. J. Cox, E. Skellam, *Org. Lett.* **2019**, *21*, 4163.
[73] M. D. Kagho, K. Schmidt, C. Lambert, T. Kaufmann, L. Jia, J. Faix, K. Rottner, M. Stadler, T. Stradal, P. Klahn, *J. Nat. Prod.* **2024**, *87*, 2421.
[74] U. B. Nair, P. B. Joel, Q. Wan, S. Lowey, M. A. Rould, K. M. Trybus, *J. Mol. Biol.* **2008**, *384*, 848.
[75] R. V. Nair, S. Zhao, E. Terriac, F. Lautenschläger, J. H. R. Hetmanski, P. T. Caswell, A. del Campo, ChemRxiv **2020**, 10.26434/chemrxiv.12609545.v1.
[76] O. A. Okoh, P. Klahn, *ChemBioChem* **2018**, *19*, 1668.
[77] X. Li, Z. Liu, A. Zhang, C. Han, A. Shen, L. Jiang, D. A. Boothman, J. Qiao, Y. Wang, X. Huang, Y.-X. Fu, *Nat. Commun.* **2019**, *10*, 3251.
[78] C. C. Jimidar, J. Grunenberg, B. Karge, H. L. S. Fuchs, M. Brönstrup, P. Klahn, *Chem. – A Eur. J.* **2022**, *28*, e202103525.
[79] A. S. Skwarecki, J. Stefaniak-Skorupa, M. G. Nowak, *Chem. – A Eur. J.* **2025**, *31*, e202403486.
[80] R. D. Rohde, H. D. Agnew, W. S. Yeo, R. C. Bailey, J. R. Heath, *J. Am. Chem. Soc.* **2006**, *128*, 9518.
[81] M. Faig, M. A. Bianchet, P. Talalay, S. Chen, S. Winski, D. Ross, L. M. Amzel, *Proc. Natl. Acad. Sci. U. S. A.* **2000**, *97*, 3177.
[82] D. L. Gustafson, D. Siegel, J. C. Rastatter, A. L. Merz, J. C. Parpal, J. K. Kepa, D. Ross, M. E. Long, *J. Pharmacol. Exp. Ther.* **2003**, *305*, 1079.
[83] M. A. Bianchet, M. Faig, L. M. Amzel, *Methods Enzymol.* **2004**, *382*, 144.
[84] T. E. Schroeder, *Zeitschrift für Zellforsch. und Mikroskopische Anat.* **1970**, *109*, 431.
[85] J. A. Spudich, S. Lin, *Proc. Natl. Acad. Sci. U. S. A.* **1972**, *69*, 442.
[86] D. J. Webb, H. Zhang, A. F. Horwitz, *Methods Mol. Biol.* **2005**, *294*, 3.
[87] A. Grada, M. Otero-Vinas, F. Prieto-Castrillo, Z. Obagi, V. Falanga, *J. Invest. Dermatol.* **2017**, *137*, e11.
[88] C. Dahlgren, H. Björnsdottir, M. Sundqvist, K. Christenson, J. Bylund, *Methods Mol. Biol.* **2020**, *2087*, 301.
[89] S. A. Belambri, L. Rolas, H. Raad, M. Hurtado-Nedelec, P. M. Dang, J. El-Benna, *Eur. J. Clin. Invest.* **2018**, *48*, e12951.
[90] H. Fu, J. Karlsson, J. Bylund, C. Movitz, A. Karlsson, C. Dahlgren, *J. Leukoc. Biol.* **2006**, *79*, 247.
[91] A. J. Jesaitis, J. O. Tolley, R. G. Painter, L. A. Sklar, C. G. Cochrane, *J. Cell. Biochem.* **1985**, *27*, 241.
[92] A. Dahlstrand Rudin, A. Khamzeh, V. Venkatakrishnan, A. Basic, K. Christenson, J. Bylund, *Cell. Microbiol.* **2021**, *23*, e13348.
[93] S. R. Punganuru, H. R. Madala, V. Arutla, R. Zhang, K. S. Srivenugopal, *Sci. Rep.* **2019**, *9*, 8577.
[94] I. Dagogo-Jack, A. T. Shaw, *Nat. Rev. Clin. Oncol.* **2018**, *15*, 81.
[95] F. Giugliano, C. Corti, P. Tarantino, F. Michelini, G. Curigliano, *Curr. Oncol. Rep.* **2022**, *24*, 809.
[96] B. Menezes, J. J. Linderman, G. M. Thurber, *Drug Metab. Dispos.* **2022**, *50*, 8.
[97] R. Kretz, L. Wendt, S. Wongkanoun, J. J. Luangsa-ard, F. Surup, S. E. Helaly, S. R. Noumeur, M. Stadler, T. E. B. Stradal, *Biomolecules* **2019**, *9*, 73.
[98] C. Lambert, M. J. Pourmoghaddam, M. Cedeño-Sanchez, F. Surup, S. A. Khodaparast, I. Krisai-Greilhuber, H. Voglmayr, T. E. B. Stradal, M. Stadler, *J. Fung.* **2021**, *7*, 131.
[99] N. Branda, *JoVE Sci. Educ. Database. Org. Chem.* **2019**.
[100] W. C. Still, M. Kahn, A. Mitra, *J. Org. Chem.* **1978**, *43*, 2923.
[101] C. C. Jimidar, C. S. G. Ganskow, M. D. Kagho, A. Chakrabarti, M. Zollo, U. Beutling, L. C. Cesar, J. Morud, M. Brönstrup, S. A. Sieber, S. M. Hacker, P. Klahn, *ChemRxiv* **2024**, 10.26434/chemrxiv-2024-f8z8z-v2.
[102] K. Becker, A.-C. Wessel, J. J. Luangsa-ard, M. Stadler, *Biomolecules* **2020**, *10*, 805.
[103] A. Chakrabarti, C. S. G. Ganskow, M. D. Kagho, C. C. Jimidar, L. Wiese, N. Beyazit, U. Beutling, M. Seeger, S. Smits, S. Nyström, A. Farewell, A. Schallmey, M. Brönstrup, P. Klahn, *ChemRxiv* **2025**, 10.26434/chemrxiv-2025-6xhv5.
[104] A. Brand, L. Allen, M. Altman, M. Hlava, J. Scott, *Learn. Publ.* **2015**, *28*, 151.